NANOPARTICLE-BASED CELLULAR MACHINERY FOR THE DEGRADATION OF SPECIFIC RNA AND PROTEIN

By

SOON HYE YANG

A THESIS PRESENTED TO THE GRADUATE SCHOOL
OF THE UNIVERSITY OF FLORIDA IN PARTIAL FULFILLMENT
OF THE REQUIREMENTS FOR THE DEGREE OF
MASTER OF SCIENCE

UNIVERSITY OF FLORIDA

2011

To my family

ACKNOWLEDGMENTS

I would like to primarily acknowledge my advisor, Dr. Charles Cao, for his the greatest guidance. I would like to also thank other committee members, Dr. Charles Martin, Dr. Jon Stewart, Dr. Nicolas Polfer and Dr. Shouguang Jin.

Finally, I would like to thank my husband, Youngmin Yoon, for his dedication to me. I am always happy because of him. He is my greatest present. I love you.

TABLE OF CONTENTS

page

LIST OF TABLES

LIST OF FIGURES

Abstract of Thesis Presented to the Graduate School
of the University of Florida in Partial Fulfillment of the
Requirements for the Degree of Master of Science

NANOPARTICLE-BASED CELLULAR MACHINERY FOR THE DEGRADATION OF SPECIFIC RNA AND PROTEIN

By

Soon Hye Yang

August 2011

Chair: Charles Y. Cao
Major: Chemistry

Nanoparticles (NPs) have been extensively studied as a novel tool for biomedicines via their unique characters such as non-toxicity, ready functionality and biomedical imaging[1-9]. This research is for a new design of gold nanoparticles (AuNPs) which specifically degrade a target RNA or protein as a medicine. By immobilizing ssDNA and an enzyme which degrades bounded target molecules on the surface of AuNPs, this research demonstrated a novel concept of nanozyme medicine. Oligonucleotide-functionalized AuNPs was used as the sensory platform for target molecules binding. Induced target molecules recognized from recognition groups could be degraded from adjacent immobilized non-specific enzymes.

Firstly, RNA silencing is a fundamental gene regulation mechanism in the cell[22, 23]. Here we report the synthesis of a nanoparticle complex capable of effectively mimicking the function of an active RNA-induced gene silencing complex (RISC)[24]—the cellular machinery that mediates the RNA interference (RNAi) pathways. Our results show that this nanoparticle complex displayed potent antiviral activity against hepatitis C virus *in vitro*. Since the function of the nanoparticle complex does not rely on cellular RNAi machinery, the RNA silencing approach herein complements those RNAi methods and

has the potential to become a useful tool for functional genomics and for combating protein expression-related diseases such as viral infections and cancers.

Secondly, as a blood coagulation enzyme, thrombin has been widely studied for coagulation disorders that are highly related to many serious heart diseases. In this study, we developed artificial anti-coagulant for thrombin based on aptamer modified AuNPs. Incubation time of the nanozymes with target molecules versus relative concentration of thrombin showed the effect of the nanozymes on the degradation of thrombin. For sequence specific study, 15-mer thrombin aptamer (GGT-TGG-TGT-GGT-TGG), three bases changed ssDNA (GGT-TGG-TGT-GGT-AAA T20) and polyT30 (TTT-TTT-TTT-TTT-TTT-TTT-TTT-TTT-TTT-TTT) functionalized nanozymes have been investigated for thrombin degradation. To test the selectivity of nanozymes for thrombin, plasmin and Rnase A were analyzed at the same conditions as those used for thrombin. Furthermore, enzyme kinetic studies of nanozymes were examined through the values of K_m, V_{max} and K_{cat} compared to native-proteinase K. Consequently, this new design of AuNPs by immobilizing ssDNA and proteinase K showed great selectivity toward thrombin. Its enzyme kinetic constants (K_m: 0.072 μM, K_{cat}: 0.003 /s, K_{cat}/K_m: 44282 /sM) compared to those of native proteinase K (K_m: 0.845 μM, K_{cat}: 0.034 /s, K_{cat}/K_m: 40393 /sM) indicated that even though nanozymes had lower enzyme kinetic efficiency than native proteinase K catalysis due to aptamer jungle on the surface of AuNPs, immobilized thrombin aptamer allows nanozymes to have 11 times higher substrate binding affinity.

CHAPTER 1
INTRODUCTION

Nanoparticles (NPs) have been extensively developed for drug and gene delivery[1-3], and biomedical imaging[4-7]. Since NPs are known as non-toxic carriers[1, 2], NP-based delivery system has been widely studied for therapeutic agents[8, 9]. This system is able to recognize target biological molecules in the human body to deliver drugs for cancer cells by using target-specific probe on their surface. Biomedical imaging techniques allow NP-based delivery systems to trace the location of drugs in a patient's body[1, 2, 4]. Varying range size and ready functionality of NPs allow them to be a useful scaffold for efficient recognition and delivery of biomolecules. A number of studies have been investigated for NPs-protein complex[10, 11] and NPs-DNA complex [12-17] for biosensors or biomedicines.

Uses of enzymes as medicine have been widely studied in industry. For example, collagenase is used for local applications. Pancreatic enzyme supplements such as chymotrypsin, trypsin, pantreatin, and panrelipase are most common pancreatic supplements used in digestive disorders[18-20]. The enzyme streptokinase is administered to patients as soon as possible after the onset of a heart attack. It minimizes the damaged heart muscle acting medically as 'fibrinolytics' by producing extra plasmin which breaks down fibrin, the major constituent of blood clots. A major application of enzymes as medicine is for cancer treatment. Studies have shown asparaginase works as for the treatment of acute lymphocytic leukaemia in children[18, 19]. However, short effective life (few minutes) of most enzymes in the circulatory system, difficulty of distribution due to their large molecular size, and eliciting immune response in the patient from prolonged use limit the uses of enzymes in medicine[21].

In order to overcome these limitations, this study uses, a simple artificial nanoparticle complex (called nanozyme) consisting of a nanoparticle, non-sequence specific endonuclease or protease, and single-stranded DNA oligonucleotides. This nanozyme has been developed to degrade a target RNA or protein. A newly designed nanozyme would be expected to have a long-life span, and to not have immune response due to the non-toxic jungle of ssDNA, and to be easy to be traced the location of the nanozyme medicine in the human body.

CHAPTER 2
NANOPARTICLE-BASED CELLULAR MACHINERY FOR THE DEGRADATION OF SPECIFIC RNA

RNA silencing is a fundamental gene regulation by which the expression of genes is suppressed by an antisense RNA molecule. RNA interference (RNAi) is the most common example of antisense RNA molecules, which is a sequence-specific RNA silencing mechanism. This mechanism is derived by small interfering RNAs (siRNAs) through the action of an endonuclease-containing protein complex known as RNA-induced silencing complex (RISC) or expressed microRNA, where the degradation of complementary messenger RNAs is induced[22-24].

The use of RNAi to control gene expression has emerged as a basic experimental tool for studying gene function and biological pathways in living cells and living organisms including plants and animals[22, 23]. Exogenous siRNA-based RNAi techniques have the potential to provide powerful therapeutic approaches for human diseases, and a number of siRNA-based therapies are currently being evaluated in clinical trials[24, 25]. However, because the therapeutic effects of siRNA drugs depend on cellular RNAi machineries, this therapeutic intervention can perturb natural cellular gene regulation pathways mediated by endogenous microRNAs that also rely on these cellular machineries, thus resulting in potential toxicity and side effects[24, 26, 27]. In addition, the therapeutic effects of siRNA can be inhibited by RNAi suppressors that are encoded by pathogenic human viruses such as hepatitis C virus (HCV) and HIV[28, 29]. Moreover, delivery of siRNA drugs into cells or tissues poses another major challenge to its clinical applications[24, 27].

Here, we report a nanozyme-based RNA-silencing approach that has the potential to overcome the difficulties associated with the use of siRNA-based drugs. In

this study, we use a nanoparticle as the backbone of the nanozyme, providing a large surface area to hold endoribonucleases and DNA oligonucleotides at close proximity. Endoribonucleases are the catalytically active components of the nanozyme, while DNA oligonucleotides function as the components responsible for target recognition via Watson-Crick base pairing and direct the endoribonucleases to cleave target RNAs that contain complementary sequences (Figure 2-2). Owing to their low toxicity and unique surface chemical properties for alkylthiol functionalization[31, 32], gold nanoparticles are chosen to construct nanozymes. RNase A is used as the endoribonuclease component because it is one of the most robust and active endoribonucleases for non-sequence specific degradation of single-stranded RNAs, which have routinely been used for the removal of RNA contamination from DNA preparations as well as the removal of unhybridized regions of RNA from DNA/RNA or RNA/RNA hybrids[23].

HCV was chosen as a model system to evaluate the function and efficacy of nanozymes for silencing gene expression and suppressing viral replication. HCV is a major cause of liver diseases such as chronic hepatitis, cirrhosis and liver cancers[32]. More than 170 million people are infected by HCV worldwide[33]. Current interferon-based therapy results in sustained virus clearance in only around 50% patients, while the therapy is not HCV-virus specific and has significant side effects. In the absence of an effective vaccine, more specific antiviral therapies are urgently needed[33, 34].

HCV is a positive-strand RNA virus and has six major genotypes and numerous subtypes[35]. The 5’ nontranslated region (5' NTR) in the HCV genome is highly conserved among the six major genotypes and this region contains an important structure known as the internal ribosome entry site that controls the initiation of HCV-

RNA translation[36]. Previous reports have shown that by targeting RNA genomic region, siRNAs can effectively inhibit the replication of HCV in cultured cells. Therefore, we chose this HCV genomic region as the nanozyme target and synthesized alkylthiol-terminated DNA oligonucleotides containing an 18 nucleotide (nt)-long fragment with sequence complementary to that of the region (nt 322–339) in the HCV genome (Figure 2-2).

Experimental Section

Materials

Thiol-modified anti-HCV DNA oligonucleotides were purchased from Bio-synthesis Inc. RNase A (ribonuclease A from bovine pancreas), RNase-free buffers, and chemicals were ordered from Sigma-Aldrich.

Synthesis of Nanozyme

Citrate-stabilized gold nanoparticles (12.5 nm in diameter with a relative standard deviation of 8%, Figure 2-1) were prepared according to literature procedures[37].

Gold nanoparticles (10 nM, 12.5 nm in diameter with a relative standard deviation of 8%) were mixed with RNase A (0.5 μM) in a carbonate buffered solution (2 mL; carbonate, 10 mM; pH 9.6)[38, 39]. Under shaking for 30 min, alkylthiol-modified anti-HCV oligonucleotides (6.4 nmol, Figure 2-2) and phosphate buffer (1.0 M, pH 7.4) were added to bring the mixture solution with 10 mM phosphate. After 8 h shaking, sodium chloride (1.5 M solution in RNase-free water) was added to bring the NaCl concentration gradually to 0.3 M during a period of 32 h. The solution was further shaken for another 8 h. Then the resulting nanozyme particles were centrifuged (13000 rpm, 20 min, for three times) and redispersed in RNase-free water. In addition, the number of RNase A loaded onto individual nanozymes can be controlled by varying the

concentration of RNase A. Note that all the vials and tubes used herein were modified by silane for minimizing the nonspecific binding of RNase A onto the glass surface of these glass containers.

Synthesis of RNA Substrates Using *in vitro* Transcription

The pJFH1 plasmid was a gift from Dr. Takaji Wakita (National Institute of Infectious Diseases, Tokyo, Japan)[40]. The human AAT gene was amplified from a patient liver tissue and cloned into pEF6/V5-His-TOPO vector (Invitrogen). The expression vector pTOPO-AAT was sequenced using the BigDye Terminator V3.1 Kit from Applied Biosystems (Foster City, CA). The pJFH1 was cut by using Cla I, and the pTOPO-AAT was cut by Xba I. The resulting linearized DNA plasmids were purified and used as the templates for *in vitro* transcription to make the HCV RNA segment (nt 1-1149) or the 1257-nt AAT RNA using MEGAscript T7 kit (Ambion, Austin, TX).

Rnase A Activity Assay

In a typical test, RNA substrates (0.5 μg) were incubated with nanozyme (0.034 nM), or Au-DNA conjugates (0.034 nM), or particle-free RNase A (0.408 nM) in a phosphate buffered saline solution (11 μL; phosphate, 10 mM; NaCl, 0.138 M; and KCl, 0.027 M) for 15 min. Then the formaldehyde loading buffer (11 μL, purchased from Londa Rockland, Inc.) was added to denature the RNA products, and the resulting solution was heated at 65 °C for 11 min, and then immediately placed on ice for 2 min before loading onto a 2% agarose/formaldehyde denaturing gel (10X MOPS buffer, 5 mL: RNase free water, 45 mL; agarose, molecular biology grade, 1.0 g; and 37% formaldehyde solution, 0.9 mL). Gel electrophoresis was performed at 60 V for approximately 90 min or until the front line of bromophenol blue dyes migrated about 6 cm in the gel. Afterwards, the gel was stained by SYBR Green II for visualization.

Proteinase K Resistance Tests

In a typical proteinase K resistance test, nanozymes (0.034 nM) or particle-free RNase A (0.408 nM) was first incubated with proteinase K (10 nM) in a PBS buffer (pH 7.4) at 37 ^{o}C for 1 h. Then the product of this proteinase K treatment was divided into two parts and further incubated with the HCV (or AAT) RNA (0.12 μM) in a PBS buffer (11 μL; pH 7.4) at 37 ^{o}C for 15 minutes. The products were analyzed by using electrophoresis in a 2% formaldehyde agarose gel as described above.

Results and Discussion

To assess the target specificity of the anti-HCV nanozyme, we performed an *in vitro* RNase activity assay with gold nanoparticle-oligonucleotide conjugates (Au-DNA, Figure 2-2c) as a negative control, and particle-free RNase A as the positive control. The target substrate was an HCV RNA segment (nt 1–1149) that contains the entire 5'NTR region of the HCV RNA genome of the HCV JFH-1 strain. The control substrate was a 1257-nt RNA segment of human alpha-1 antitrypsin (AAT) gene that does not contain complementary sequences to the nanozyme-bearing oligonucleotides. The HCV (or AAT) RNA (0.12 μM) was incubated with the anti-HCV nanozymes or a control in a phosphate-buffered saline solution (PBS, 11 μL; pH 7.4) at 37 ^{o}C for 15 minutes, and the corresponding products were analyzed by electrophoresis in a denaturing agarose gel.

Electrophoresis analyses show that while the anti-HCV nanozyme displayed no measurable cleavage activity on the AAT RNA, it did cleave the HCV RNA target into two major fragments with a size of about 300 nt and 800 nt, respectively (Figure 2-3). Amazingly, this result corresponds to a cleavage site fully matching the predicted

position where the HCV RNA binds to the nanozymes via DNA/RNA hybridization (Figure 2-2). On the contrary, Au-DNA conjugates showed no cleavage activity against either the HCV or AAT RNA, whereas unbound RNase A degraded both RNA substrates into short fragments, which appeared as broad smear bands (Figure 2-3). Together, these results demonstrate that the anti-HCV nanozyme exhibits remarkable target specificity and displays a RISC-like function—cleaving its target RNAs in a sequence- and site-specific manner (Figure 2-2).

We attribute this RISC-like function to the cooperative coupling between the RNase and DNA-oligonucleotide components of the nanozyme (Figure 2-2). On one hand, the access of non-complementary RNAs to the nanozyme-bearing RNase molecules is likely blocked by the densely packed oligonucleotides through steric hindrance and repulsive coulomb interactions. On the other hand, these DNA oligonucleotides can also bind to target RNAs via base pairing and bring them to the RNase molecules on the nanozyme, resulting in the endonucleolytic cleavage of these RNAs into two fragments at positions close to the binding site (Figure 2-2 and 2-3).

Given the potential for RNase A degradation by proteinases in the cell or *in vivo*[41], we next examined the *in vitro* resistance of the anti-HCV nanozyme against proteinase K compared with particle-free RNase A (Figure. 2-3). RNase activity tests show that unbound RNase A lost its activity almost completely after the incubation with proteinase K in a PBS buffer (pH 7.4) at 37 ^{o}C for 1 h. In contrast, nearly no measurable change was observed in the nanozyme activity after an identical proteinase K treatment (Figure. 2-3). We attribute the resistance to proteinase degradation to the fact that the RNase molecules on the nanozyme were protected by the tightly packed

oligonucleotides (Figure. 2-2). The ability to resist proteinase degradation should enhance the stability of these nanozymes in the cell and *in vivo.*

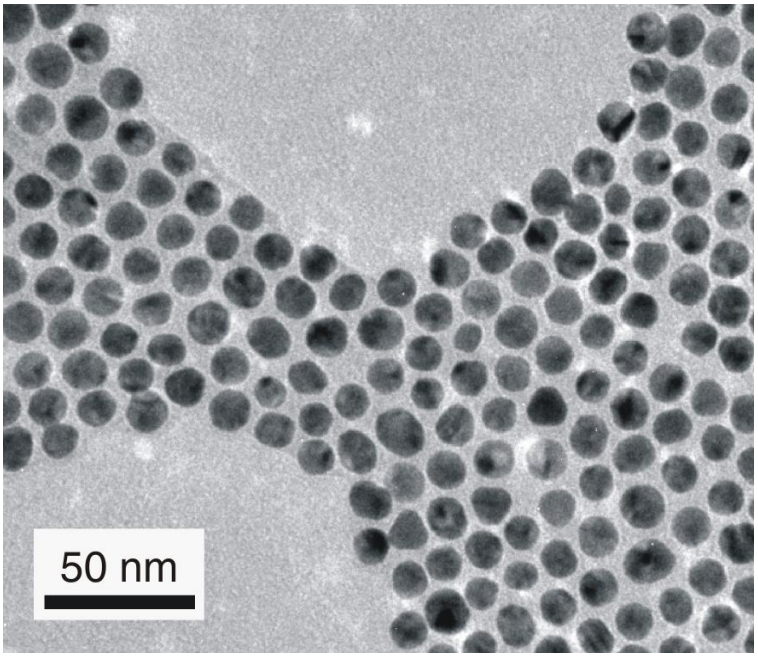

Figure 2-1. TEM image of Au nanoparticles

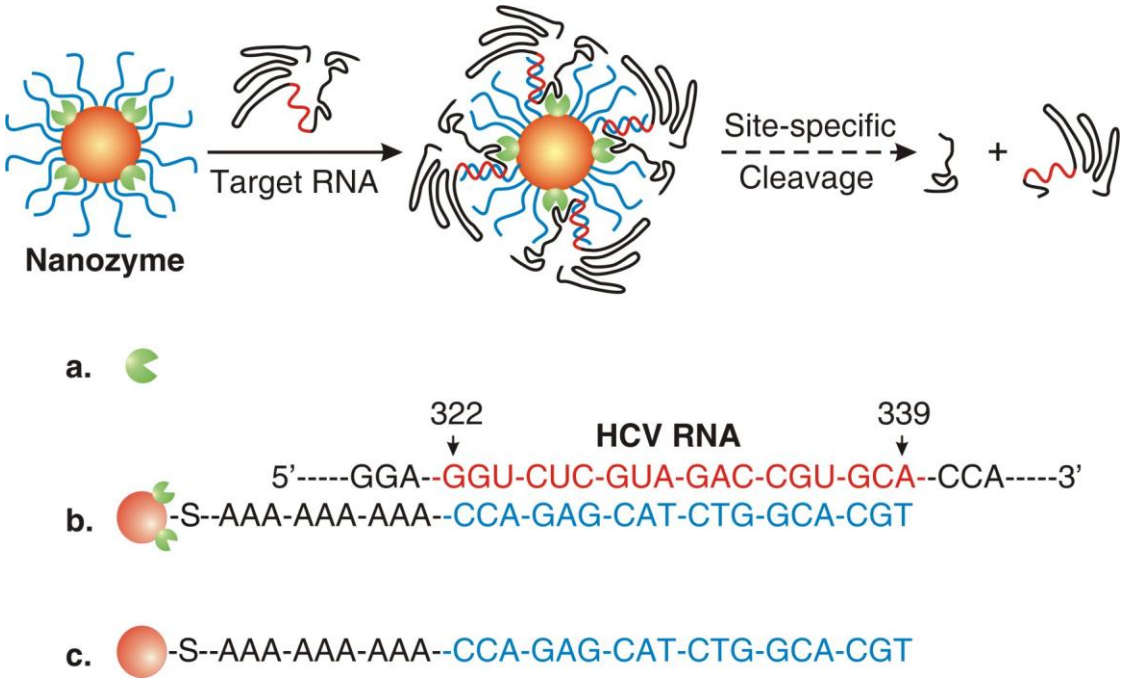

Figure 2-2. Schematic representation describing the design and function of nanozyme. (A) Shown is an endoribonuclease. (B) Nanozyme-bearing DNA oligonucleotides complementary to the sequence at the HCV RNA position (322-339 nt). (C) Gold nanoparticle-DNA oligonucleotides conjugate (Au-DNA), a nanozyme counterpart that does not bear endoribonucleases.

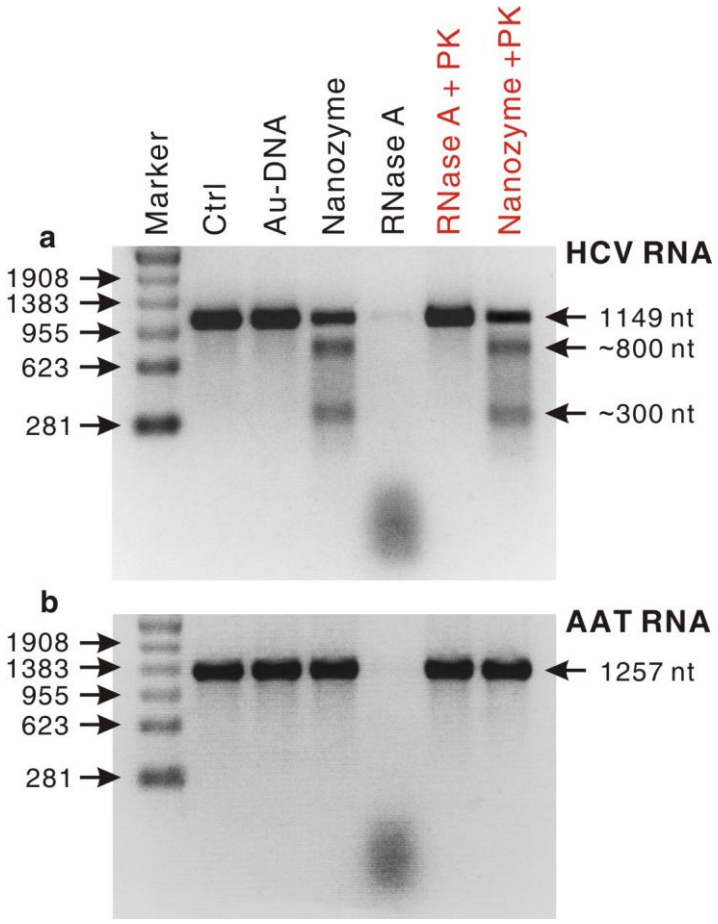

Figure 2-3. Ribonuclease activity tests for assessing the target selectivity of anti-HCV nanozyme and its ability to resist the degradation of proteinase activities. (A) HCV-RNA segment (nt 1-1149) as the substrate. (B) 1257-nt AAT RNA segment as the substrate. Abbreviations: Ctrl stands for blank control; and PK for proteinase K.

CHAPTER 3
NANOPARTICLE-BASED CELLULAR MACHINERY FOR THE DEGRADATION OF SPECIFIC PROTEIN

Coagulation disorders are highly related to many serious diseases including heart attacks and strokes[43]. Bacause thrombin can form blood clots, thrombin, consequently, became a typical target protein for anti-coagulation therapies[44-46].

In a pathological situation, excessive amount of protease or inactivation of inhibitory activity is able to interrupt inhibitory functions of anti-coagulants[47]. Inflammation caused by tissue damages or infection depends on proteolytic enzymes, plasma cascade systems, including thrombin[48]. Imbalance between proteases and their inhibitory regulators lead to the multiple organ failure. Moreover, thrombin activity imbalance in the brain may cause neurodegenerative diseases[49].

In 2006, the American Heart Association reported that prevalence rate of coronary heart disease were 17.6M in the United States[50]. As an important enzyme in the coagulation process, thrombin activity is an issue during coronary artery bypass surgery, percutaneous coronary intervention and heart transplantations. And, an anti-thrombin agent or agent that is able to inhibit thrombin activity has been used as an anti-coagulant during these surgeries. The National Center for Health Statistics estimates that in 2006, 448,000 coronary artery bypass procedures were performed on 253,000 patients in the United States[50].

Heparin is the most common anti-coagulant which can bind to exosite II on thrombin, and then it indirectly inhibits thrombin activity, because heparin strongly catalyzes the function of anti-thrombin[51]. Since heparin must be used with the antidote protamine, heparin-protamine treatment leads to a number of side-effects including bleeding and platelet count reduction. In addition, heparin has a number of

disadvantages including non-specific binding to plasma proteins, unable to inhibit clot-bound thrombin and dosing difficulty due to non-linear kinetics[52, 53]. In addition to natural thrombin inhibitors, newly designed approaches have shown to develop thrombin inhibitors, such as nucleotide-based thrombin inhibitor (thrombin aptamer)[54-56]. Nevertheless, an engineering of oligonucleotide based aptamer and a study for enhancement of its performance still remain for investigation.

Thus, there is a demand for a development of safe, long-lasting and moderate-cost anti-coagulant which is not associated with the side effects.

Human α-Thrombin

α-thrombin is a multifunctional serine protease that produces insoluble fibrin through selective cleavage of Arg-Gly bonds of soluble fibrinogen[57-59]. The polymerized fibrin is held together by noncovalent and electrostatic forces and stabilized by the transamidating enzyme, factor XIIIa that is produced by the action of thrombin on factor XIII. The insoluble fibrin aggregates and aggregated platelets then block the damaged blood vessel and prevent further bleeding. In addition, active protease-activated receptors play a pivotal role in the pathogenesis of clinical disorders[60, 61]. The concentration of thrombin is to be concerned in pathological conditions including central nervous system injury, thromboembolic disease, and Alzheimer's disease. A normal adult generates 300 nM of thrombin when he/she is injured. This thrombin survives a few minute in the body. Low concentrations of thrombin mediate neuroprotection against ischemia and environmental insults such as oxidative stress, hypoglycemia, hypoxia, and growth supplement deprivation. High concentrations of thrombin, however,

are shown to cause degeneration and cell death in both astrocyte and hippocampal neuron[62, 63].

Thrombin is consists of two polypeptide chains (A and B chain) that are covalently linked through a disulfide bond. The A chain is not responsible for proteolytic activity of thrombin (36 residues), but the B chain (259 residues) allows thrombin to act as a serine protease[64-66]. The active site contains His 57, Asp 102, and Ser 195, which performs cleavage of thrombin substrate on arginine residues. There are two extended surfaces on thrombin, composed of positively charged residues (exosite I and II)[67-70]. Exosite I binds to thrombin substrates (fibrinogen, thrombin receptor, heparin cofactor II) and ligands (thrombomoduline, glycoprotein 1b). Exosite II is a polyanionic binding site such as heparin and prothrombin fragment.

Thrombin Aptamer

Aptamers are nucleic acid molecules which have highly specific binding affinity to selected molecules with broad range of targets from ions to proteins. The SELEX method (systematic evolution of ligands by exponential enrichment) allows the aptamers to be produced by in vitro process[71, 72]. A typical aptamer has 10-15 kDa molecular weights (30-45 nucleotides), and binding affinity with its target molecules is sub-nanomolar[73-75].

Aptamers have been used for therapeutics and diagnostics because of their high selectivity and affinity, as well as biological functions[75-77]. Since the synthesis of aptamers and labeling of aptamers is simple, their secondary structures are easily predicted. In addition, aptamers are not prone to the irreversible denaturation. These advantages in the utilization of aptamers have attracted increasing interest as the biorecognition element in biosensors and drug delivery systems[78-81]. Moreover, they

have several advantages over antibodies and other protein biologics. First, in-vitro production of aptamers allows rapid generation of aptamers, and selectivity and affinity of aptamers to be controlled. Second, aptamers are non-toxic, and do not trigger immune response. Third, aptamer's small size and ready functionality of end residue with a variety of functional groups allows them to be easily immobilized on the surface of nanoparticles. Fourth, since therapeutic aptamers are chemically produced, they can be readily scaled-up with a relatively lower cost than that of antibodies. Finally, aptamers are very stable from heat and denaturants allowing them to be stored more for than 1 year at room temperature.

In this study, 15-mer thrombin aptamer (GGT-TGG-TGT-GGT-TGG) which is known as the first DNA aptamer isolated from *in vivo* selection was used. 15-mer thrombin aptamer (15-TBA) is binding to exosite I of thrombin, and its dissociation constant (Kd) is relatively high (100 ~ 450 nM), depending on measurement methods[76, 82, 83].

15-TBA has been extensively used for thrombin biosensors. Most of the biosensors based on aptamer take advantage of target-induced conformational change of the aptamer, which causes electrochemical[84, 85], fluorescence[86, 87], absorbance[88], colorimetric[89, 90], and surface-enhanced Raman scattering (SERS) signals[91, 92]. These aptasensors are based on DNA aptamer complementary sequence complex tagged with a fluorophore or an electrochemical moiety. It is also based on conformational change of a single-stranded aptamer built on AuNPs used in colorimetric, electrochemical, and SERS sensors or using immobilized aptamer, which has multiple binding sites, on AuNPs for sandwich type biosensors. Because 15-TBA interacts with

the fibrinogen–binding exosite I, 15-TBA is able to inhibit the thrombin activity[44, 45, 68]. Therefore, there were several approaches that utilized 15-TBA as a potential anti-coagulant[54, 55]. Only limited progress has been made, however, in the use of 15-TBA as an anti-coagulant due to its low strength of binding with thrombin exosite I[76, 82, 83].

Proteinase K

Proteinase K (PK) is a serine protease and its predominant site of cleavage is the peptide bond adjacent to the carbonyl group of aliphatic and aromatic amino acids with blocked alpha amino groups. The enzyme is named because of the enzyme's ability to digest keratin. Its broad substrate specificity, high activity, and ability to digest native proteins result in PK being considerably useful in procedures where the inactivation and degradation of protein is required, particularly in the process for purification of nucleic acids. PK has been adapted for degradation of thrombin due to its strong ability to digest most of proteins non-specifically. PK is very stable at high temperatures, and it has wide stable pH range (from 4 ~ 9)[93, 94].

Basic Enzyme Kinetics

An enzyme reaction is used to be processed in two-steps: substrate (S) and enzyme (E) binding for formation of an enzyme-substrate (ES) complex, following irreversible enzyme-substrate decomposition to free enzyme and product (P):

$$E + S \underset{k_{-1}}{\overset{k_1}{\rightleftharpoons}} ES \xrightarrow{k_{cat}} E + P \qquad k_d = \frac{k_{-1}}{k_1}$$

Initially in an enzyme and the substrate reaction, reaction velocity is directly proportional to the amount of substrate following first-order reaction. Once the enzyme

is saturated with the substrate, rate of reaction is independent to the substrate concentration (Figure 3-1).

There are three utilities for enzyme kinetic analysis: elucidating enzyme mechanism and comparing between enzymes, predicting enzyme activity under various conditions and developing enzyme inhibitors (or activators) as therapeutic agents.

In the steady-state model assumption, the concentration of enzyme-substrate complex (ES) remains constant in time. From this assumption, Michaelis-Menten equation is derived:

$$V = \frac{V_{max}[S]}{K_m + [S]}$$

And, Michaelis-Menten constant (K_m) is equivalent to the dissociation constant of the ES complex when $k_{cat} << k_{-1}$:

$$K_m = \frac{k_{-1} + k_{cat}}{k_1}$$

The K_m corresponds to substrate concentration at $V_{max}/2$. Since the K_m is almost same as the k_d, except for the presence of the k_{cat} term, it is related to the affinity or strength of binding of a substrate to the enzyme.

$$V_{max} = k_{cat}[E_T],\ [E_T] = [E] + [ES]$$

Maximum velocity (V_{max}) is achieved at high substrate levels ($[S] >> K_m$). Thus, the entire enzyme is in the [ES] form.

Turn over number or catalytic efficiency is derived by V_{max} and the total amount of the enzyme when the enzyme is fully saturated with the substrate.

$$k_{cat} = V_{max}/[E_T]$$

k_{cat} indicates that the moles of products are produced by a single enzyme molecule in a certain period time.

To calculate the important enzyme kinetic constants, a graphical analysis of the experimental data is necessary. Since the accurate determination of V_{max} on the graph, velocity versus [S], is difficult, double reciprocal plots have been widely used via Lineweaver-Burke Plots (Figure 3-2).

$$\frac{1}{V} = \frac{K_m}{[S]}\frac{1}{V_{max}} + \frac{1}{V_{max}}$$

$y = 1/v$, $x = 1/[S]$

y-intercept = $1/V_{max}$

Slope = K_m/V_{max}

Experimentally, from the various concentration of the substrate versus recording the initial velocity, one could get Lineweaver-Burke Linear Plots.

Last important parameter of enzyme kinetics is the term of k_{cat}/K_m. It indicates the second order reaction of free E and free S. This is a significant term for describing the specificity/selectivity of the enzyme for a given substrate.

In this study, nanozyme kinetics has been examined by comparing to native proteinase K for a thrombin substrate.

Experimental Section

Materials and equipment

Thiol-modified and thrombin 15mer-aptamers (GGT-TGG-TGT-GGT-TGG T20) were purchased from Bio-synthesis Inc. Human α-thrombin and human plasmin were ordered from Heamatologic Technologies Inc., and RNase A (ribonuclease A from bovine pancreas), Proteinase K (from tritirachium album), chromogenic substrates (thrombin substrate, β-Ala-Gly-Arg-*p*-nitroanilide; plasmin substrate, H-D-Val-Leu-Lys-*p*-nitroanilide; RNase A substrate, cytidine-2',3'-phosphate) and chemicals were ordered from Sigma-Aldrich. Thiol-modified PEG (Poly Ethylene Glycol) was ordered from Laysan Bio Inc.

All acquisition of experimental data was obtained by UV-Vis absorption spectroscopy (Agilent 8453E UV-visible Spectroscopy System).

Synthesis of Nanozyme

Gold nanoparticles (5 nM, 12.5 nm in diameter with a relative standard deviation of 8%, Figure 2-1) were mixed with Proteinase K (0.2 μM) in a carbonate buffered solution (2 mL; carbonate, 10 mM; pH 9.6)[38, 39]. Under shaking for 30 min, 1.0 mM $CaCl_2$ was added then incubated for overnight at 4°C. Alkylthiol-modified thrombin 15mer-aptamer (1.0 μM) and phosphate buffer (1.0 M, pH 7.4; Tween 20, 0.01%) were added to bring the mixture solution with 10 mM phosphate. After 20 min shaking, the solutions were sonicated for 10 sec, and then sodium chloride (2.0 M solution) was added to bring the NaCl concentration gradually to 0.3 M every 20min with 10 sec sonication. Lastly, thiol-modified PEG (8.0 μM) was added. The solution was further shaken overnight at 4°C. Then the resulting nanozyme particles were centrifuged (15000 rpm, 20 min, for four times washed by 0.01% Tween 20) and re-dispersed in phosphate buffer (10 mM; NaCl,

0.154 M; KCl, 0.005 M; $CaCl_2$, 0.001 M; $MgCl_2$, 0.001 M; Glycerol, 5%; and Tween 20, 0.01%; pH 7.4). The nanozyme solution was stored in refrigerator at 4°C before use (Figure 3-3).

For quantitative analysis of a loading amount of proteinase K on nanozyme, the supernatant after the centrifugation for first washing was measured through UV-Vis absorption spectroscopy at 410 nm (proteinase K substrate, Succinyl-Ala-Ala-Ala *p*-nitroanilide, 0.5 mM) in Tris buffer (20 mM: NaCl, 0.154 M; KCl, 0.005 M; $CaCl_2$, 0.001 M; $MgCl_2$, 0.001 M; and Glycerol, 5%; pH 7.4) with 10 folds dilution.

Proteinase K Activity Assay

In a typical test, thrombin substrates (0.03 μM) were incubated with nanozymes (0.15 nM) in a phosphate buffered saline solution (1 mL; phosphate, 10 mM; NaCl, 0.154 M; KCl, 0.005 M; $CaCl_2$, 0.001 M; $MgCl_2$, 0.001 M; Glycerol, 5%; and Tween 20, 0.01%; pH 7.4) for 0 (10 min), 1, 2, 3, 4, 5, 6, 7, 8, 9 and 10 hr at 37°C. Then the solutions were centrifuged to remove the particles (15000 rpm, 30 min). The remaining amount of thrombin in a supernatant was measured through UV-Vis absorption spectroscopy at 405 nm (thrombin substrate, β-Ala-Gly-Arg-*p*-nitroanilide, 0.5 mM).

Selectivity Assay of Nanozyme

For selectivity test, thrombin (0.03 μM), plasmin (0.03 μM) and RNase A (0.2 μM) were incubated with nanozymes (0.15 nM) in a phosphate buffered saline solution (1 mL; phosphate, 10 mM; NaCl, 0.154 M; KCl, 0.005 M; $CaCl_2$, 0.001 M; $MgCl_2$, 0.005 M; Glycerol, 5%; and Tween 20, 0.01%: pH 7.4) for 0 (10 min), 1, 2, 3, 4, 5, 6, 7 and 8 hr at 37°C. Then the solutions were centrifuged to remove the particles (15000 rpm, 30 min) and the remaining amount of thrombin, plasmin and RNase A in a supernatant was measured through UV-Vis absorption spectroscopy (thrombin substrate, β-Ala-Gly-Arg-

p-nitroanilide, 0.5 mM at 405 nm; plasmin substrate, H-D-Val-Leu-Lys-*p*-nitroanilide, 0.05 mM at 405 nm; RNase A substrate, cytidine-2',3'-phosphate, 0.1 mg/mL at 286 nm).

Sequence Specific Assay of Nanozyme

The Au-nanoparticles that are immobilized with three-base modified 15mer-ssDNA (GGT-TGG-TGT-GGT-AAA T20) and Poly T30 instead of 15mer-thrombin aptamer have been used for sequence specific assay. Thrombin substrates (0.03 μM) were incubated with the ssDNA modified AuNPs(0.15 nM) in a phosphate buffered saline solution (1 mL; phosphate, 10 mM; NaCl, 0.154 M; KCl, 0.005 M; $CaCl_2$, 0.001 M; $MgCl_2$, 0.001 M; Glycerol, 5%; and Tween 20, 0.01%; pH 7.4) for 0 (10 min), 1, 2, 3, 4, 5, 6, 7 and 8 hr at 37°C. Then the solutions were centrifuged to remove the particles (15000 rpm, 30 min) and the remaining amount of thrombin in a supernatant was measured through UV-Vis absorption spectroscopy at 405 nm (thrombin substrate, β-Ala-Gly-Arg-*p*-nitroanilide, 0.5 mM).

Enzyme Kinetic Study for Nanozyme

For enzyme kinetic study, different concentrations of thrombin substrates (from 0.01 to 0.12 μM) were incubated with nanozymes (0.15 nM) in a phosphate buffered saline solution (1 mL; phosphate, 10 mM; NaCl, 0.154 M; KCl, 0.005 M; $CaCl_2$, 0.001 M; $MgCl_2$, 0.001 M; Glycerol, 5%; and Tween 20, 0.01%; pH 7.4) for 2, 4 and 6 hr at 37°C. Then the solutions were centrifuged to remove the particles (15000 rpm, 30 min). The remaining amount of thrombin in a supernatant was measured through UV-Vis absorption spectroscopy at 405 nm (thrombin substrate, β-Ala-Gly-Arg-*p*-nitroanilide, 0.5 mM).

Native proteinase K (1.0 nM) were incubated with different concentrations of thrombin substrate (from 0.05 to 1.0 μM) in a phosphate buffered saline solution (1 mL; phosphate, 10 mM; NaCl, 0.154 M; KCl, 0.005 M; $CaCl_2$, 0.001 M; $MgCl_2$, 0.001 M; Glycerol, 5%; and Tween 20, 0.01%; pH 7.4) for 2, 4 and 6 hr at 37°C. Then the solutions were measured through UV-Vis absorption spectroscopy at 405 nm (thrombin substrate, β-Ala-Gly-Arg-*p*-nitroanilide, 0.5 mM).

Results and Discussion

Proteinase K Loading Determination

The average number of proteinase K molecules loaded onto a single nanozyme was determined by a subtraction method. The total amount of proteinase K molecules loaded on to gold nanoparticles in a synthesis batch was determined by subtracting the amount of unloaded proteinase K molecules from the amount of proteinase K molecules added initially. This total loading amount was then divided by the total number of nanozymes in the solution, yielding the average number of proteinase K per single nanozyme. The number of nanozymes was determined by using UV-Vis absorption spectroscopy (λ= 524 nm, ε = 2.0×10^8 $M^{-1}cm^{-1}$). The amount of unloaded proteinase K in a reaction solution was determined by measuring the proteinase K activity of the supernatant resulted after removal of nanozymes (Table 3-1). A typical proteinase K activity measurement was performed according to the literature method, in which succinyl-Ala-Ala-Ala *p*-nitroanilide (at 410 nm) was used as the substrate[95]. Then the amount of proteinase K molecules was obtained using a standard proteinase K activity curve (Initial reaction rate as a function of proteinase K concentration: 0.05, 0.07, 0.1, 0.12 and 0.15 μM were chosen, Figure 3-4).

Nanozyme activity to thrombin

To assess the nanozymes activity to a target molecule, thrombin, an *in vitro* proteinase K assay was performed by using gold nanoparticle which is modified with proteinase K, 15mer-thrombin aptamer (GGT-TGG-TGT-GGT-TGG T20) and PEG (MW 1000). In this study, a nanoparticle as the backbone of nanozymes was used to provide a large surface area to hold protease and DNA oligonucleotides at close proximity. The recognition group could selectively bind to targets of interest, and bring them to the nearby enzymes for reaction, and therefore, well-designed recognition group make nanozymes exhibit extraordinary high target selectivity. Proteases are the catalytically active components of nanozymes, while DNA oligonucleotides function as the components responsible for target recognition and direct the proteases to cleave target proteins (Figure 3-5).

Nanozymes for thrombin target can be used as a class of a novel agent for thrombin inhibitor to regulate blood coagulation in the body. An activated nanozyme can sequence-selectively cleave thrombin, and is expected to prevent blood coagulation.

In a typical experiment, a thrombin solution (0.03 μM, pH 7.4) was mixed with a solution of nanozymes (0.03 OD/mL), in the resulting solution is 0.15 nM. This mixture was incubated at 37°C and centrifuged for removal of reacted nanozymes. The supernatants were measured through UV-Vis absorption spectroscopy at 405 nm (thrombin substrate, β-Ala-Gly-Arg-*p*-nitroanilide, 0.5 mM) for every 1 hour reaction. Under the certain concentration of nanozymes and thrombin, after first two hours, nanozymes degrade thrombin linearly, and then nanozyme efficiency was reduced gradually due to limited amount of thrombin (Figure 3-6).

Selectivity of Nanozyme

The protecting ligands (PEG) control the intracellular stability and dispersibility of nanozymes. Together with the recognition groups, the protecting ligands can also prevent non-target molecules approaching to the enzymes on nanozymes, and resulting in additional selectivity for nanozymes. Molecular weight of 1000 thiol-modified PEG was chosen for a protecting ligand of nanozymes. At first trial, 5000 of PEG was tested for protecting agent (estimated the length of PEG is 40 nm), but such a long length of PEG modified nanoparticles containing DNA olignucleotide degraded other enzymes as well, and did not have sequence selectivity to thrombin (when use Poly T30 modified gold nanoparticle, data is not shown). However, when we use 1000 PEG (estimated length is 9 nm) of which length is similar to 15mer-thrombin aptamer (GGT-TGG-TGT-GGT-TGG T20, estimated length is 9.5 nm) to make nanozymes, it showed great selectivity against plasmin and Rnase A (Figure 3-7), and three bases modified 15mer-thrombin aptamer (15mer-s) and PolyT30 immobilized gold nanoparticle did not degrade thrombin (Figure 3-8). These results indicate that PEG which has a longer length than recognition oligonucleotides might not be immobilized on Au-NPs densely due to its large molecular size. However, a similar length of PEG with recognition group seemed to effectively prevent non-specific binding due to its dense structure so that it could reduce the negative charge on nanozyme from phosphate group of ssDNA; pI of thrombin is ~7. It is known that thrombin easily binds on neutral or negative charged surface.

Enzyme Kinetics of Nanozyme

As an artificial medicine that is modified with enzyme, nanozymes would be expected that it could be studied at the point of enzyme kinetics. When a new enzyme is

developed, researchers first characterize the enzyme based on kinetic constants to evaluate the efficiency of the enzyme; Michaelis constant (K_m), V_{max}, K_{cat} and K_m/K_{cat}. To calculate these values, a velocity versus [S] graph is required. Since the natural reaction of native protinase K digestion to thrombin is very slow (hourly reaction) depends on used concentration, nanozyme or native proteinase K reaction with thrombin was processed for 2, 4 and 6 hours, and then an initial velocity was measured through the slope of these three points (Figure 3-9A and 3-10A). Since the accurate determination of V_{max} on the graph, velocity versus [S], is difficult, double reciprocal plots were used via Lineweaver-Burke Plots (Figure 3-9B and 3-10B).

From the proteinase K loading determination (one nanozyme has ~6 proteinase K), 0.15 nM of nanozymes were considered which have ~0.9 nM of proteinase K activity. Therefore, their enzyme kinetics was compared to that of 1.0 nM native proteinase K. The K_m of nanozymes (0.072 μM) compared to the native proteinase K (0.845 μM) exhibited a 12 fold higher affinity to thrombin substrate. Such a decrease in the K_m values of immobilized enzymes has been recognized previously using synthetic peptide substrate[96]. It has been explained due to electrostatic attraction of hydrophobic adsorption of the substrate to the solid it might lead to the presence of areas of increased substrate concentration around the particle. Nanozymes, however, contain the specific recognition group of oligonucleotides to targets. No one has been studied for enzyme kinetics using thrombin as a substrate of proteinase K. Therefore, first we needed to investigate the proteinase K kinetics using thrombin as a substrate, and then compare to those two enzymes by kinetic constants.

The obtained maximum velocity V_{max} of the reaction catalyzed by nanozymes was 0.010, which is 8% in comparison to native proteinase K catalysis (0.123). From a reaction rate point of view, the maximal velocity of substrate change was calculated as a remaining amount of thrombin from proteinase K digestion per hour. k_{cat} is the catalytic rate constant which indicates the catalytic efficiency of the enzymes. k_{cat} is measured as how many products (moles) are produced by one mole of enzyme at the certain period time (per second). Therefore, it is also called “turnover number” of substrate by one mole of enzyme reaction. Since V_{max} is expressed by $k_{cat}[E_T]$ ($V_{max}=k_{cat}[E_T]$), if V_{max} is known from the Lineweaver-Burke plot, one could calculate the k_{cat} by using the total enzyme concentration. From proteinase K loading determination, the total amount of enzymes on nanozymes was determined to be 0.9 nM. Therefore, nanozyme’s k_{cat} was calculated as 0.003 (/s), which is an 11 times slower reaction rate than native proteinase K catalysis (0.034 /s) to thrombin. The lower rate of enzyme reaction and catalytic efficiency of nanozymes could be due to limited diffusion of thrombin molecules to the surface of the particles and to the active sites of the immobilized enzyme, especially, to the aptamer jungle on nanozymes. Nevertheless, because of extremely low K_m value of nanozymes, nanozyme’s K_{cat}/k_m value (44282 /Ms) which describes the substrate preference, is similar to native proteinase K’s substrate preference (40393 / Ms) to thrombin target (Table 3-2).

CHAPTER 4
CONCLUSIONS

When taken together, the results presented herein provide unambiguous evidence that anti-HCV nanozymes—with a remarkably cooperative, RISC-like, gene silencing function—are effective intracellular gene regulation agents for the suppression of HCV replication. This nanoparticle-based gene regulation approach complements RNAi-based approaches and has the potential to become a useful tool for functional genomics and for combating protein expression-related diseases such as viral infections and cancers. Importantly, since the antiviral function of the nanozyme is independent from cellular RNAi machineries, nanozyme-mediated RNA silencing does not in principle interfere with naturally occurring gene regulation pathways mediated by microRNAs and cannot be inhibited by the RNAi suppressors encoded by pathogenic human viruses (*e.g.*, HCV, HIV).

In addition, the results presented herein demonstrate that nanozymes- direct thrombin inhibitors (DTIs)-like, enzyme medicine function-is a nanoparticle-based synthetic analog of enzyme medicine which exhibits high target selectivity and high enzymatic activity for an anti-coagulant in the blood as a thrombin regulation agent. 15mer-thrombin aptamer was used for recognition ligand, and non-specific digestive enzyme, proteinase K, was immobilized for thrombin degradation, and PEG was chosen for a protecting ligand. A newly designed gold nanoparticle showed highly selective and specific digestion to thrombin, and these results have been investigated by using plasmin and Rnase A for selectivity study, and three-base modified 15mer-thrombin aptamer and polyT30 immobilized nanoparticle were used for sequence specific study of nanozymes. Furthermore, enzyme kinetics of nanozymes was studied compared to

native proteinase K. Even though nanozymes had lower enzymatic efficiency than native proteinase K catalysis, because of specific recognition ligand, it showed extremely high substrate affinity and selectivity.

Moreover, this platform will allow one to add functionality that could direct nanozymes to specific tissues, organs, and even sub-cellular organelles that express target genes[2]. Furthermore, this work presents a critical step toward a new class of nanoparticle-based intercellular machineries with extraordinarily cooperative functions, remarkable target selectivity, and perhaps allosteric functions that enable these machineries to have an on/off switch in response to chosen allosteric effectors such as specific byproducts in disease-associated metabolism pathways, thus providing a powerful tool for studying and regulating a wide variety of biological pathways such as those in somatic cell reprogramming.

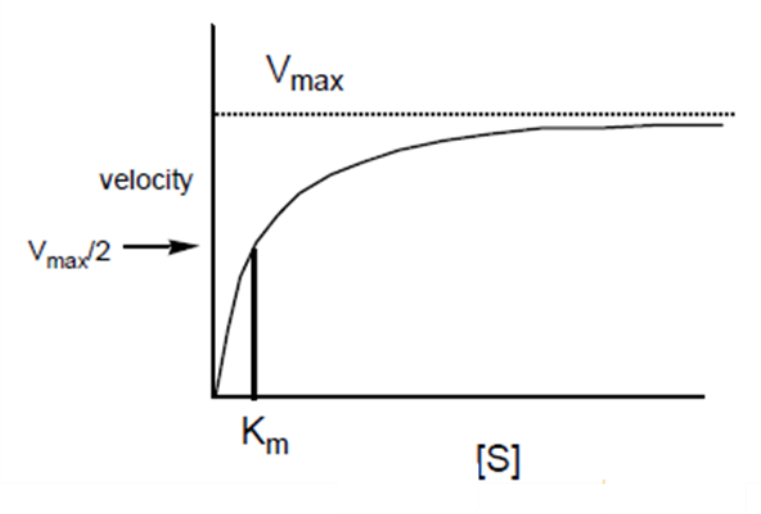

Figure 3-1. Substrate concentration versus enzyme reaction velocity.

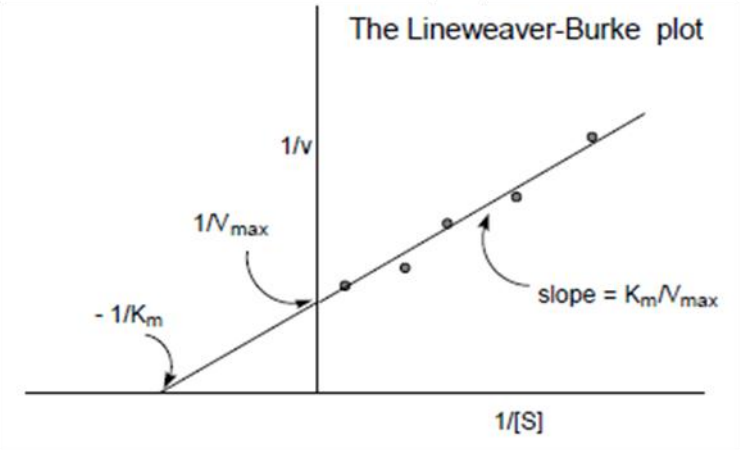

Figure 3-2. Lineweaver-Burke Plots.

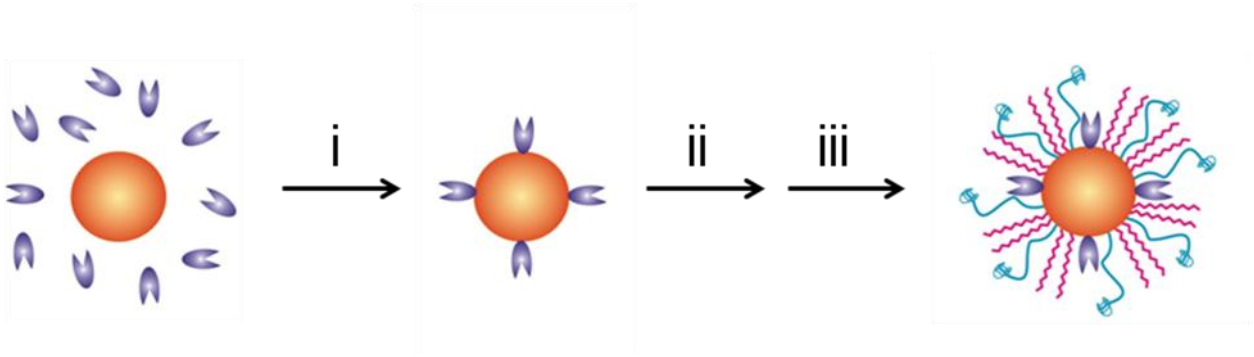

Figure 3-3. Schematic presentation of a synthesis of a thrombin-selective nanozyme: (i), loading proteinase K onto the surface of gold nanoparticles; (ii), the loading of recognition group (thrombin aptamer, GGT-TGG-TGT-GGT-TGG-T20); and (iii), the loading of protection group (PEG, MW:1000) onto the surface of gold nanoparticles.

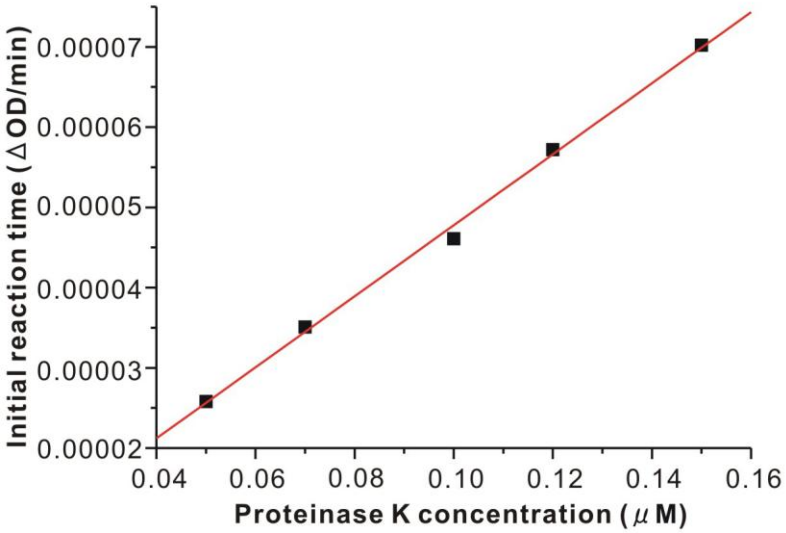

Figure 3-4. Plot of initial reaction rate as a function of Proteinase K concentration for hydrolysis of succinyl-Ala-Ala-Ala p-nitroanilide. The substrate concentration was 0.5 mM.

Table 3-1. Determination of Proteinase K loading number per gold nanoparticle

Experimental contents	Experimental results
Initial mole ratio of Proteinase K/Au	40:1
Initial reaction rate (ΔOD/min)	0.0000483
Residue amount (μM)*	0.101
Original amount (μM)	0.133
Percent loading	23.9%
Proteinase K number per Au	6.4

* The residue amount of Proteinase K was calculated using the standard curve in Figure 3-4 (Y=4.43E-4X+3.50E-6, R=0.9985).

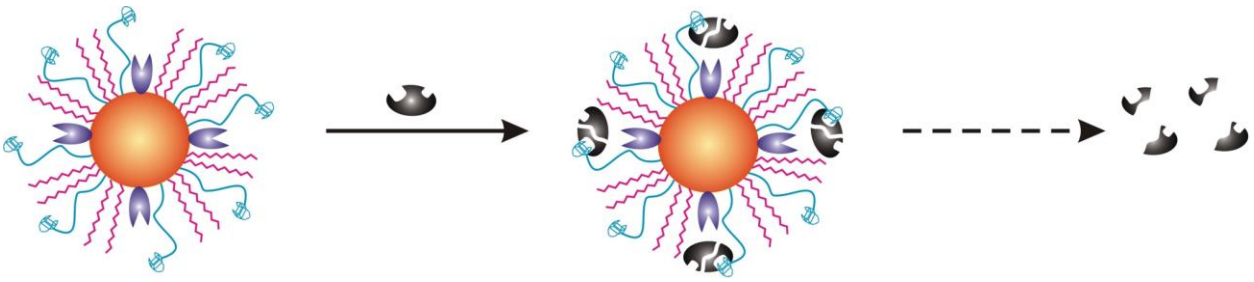

Figure 3-5. Schematic representation describing the mechanism of nanozyme reaction to thrombin.

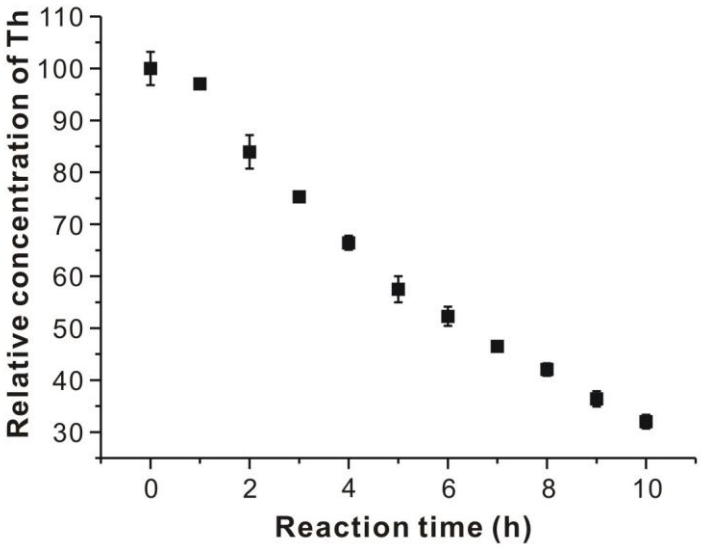

Figure 3-6. Illustration of nanozyme activity for thrombin degradation.

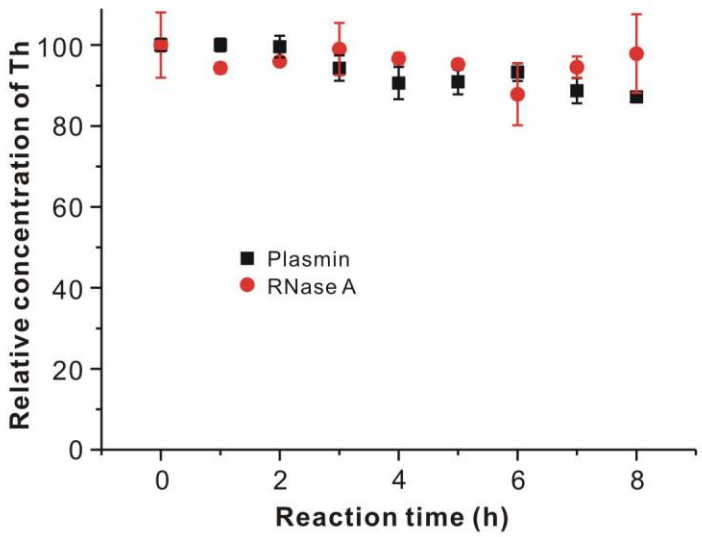

Figure 3-7. Illustration of thrombin selective nanozyme that displays no-degradation to Plasmin and Rnase A.

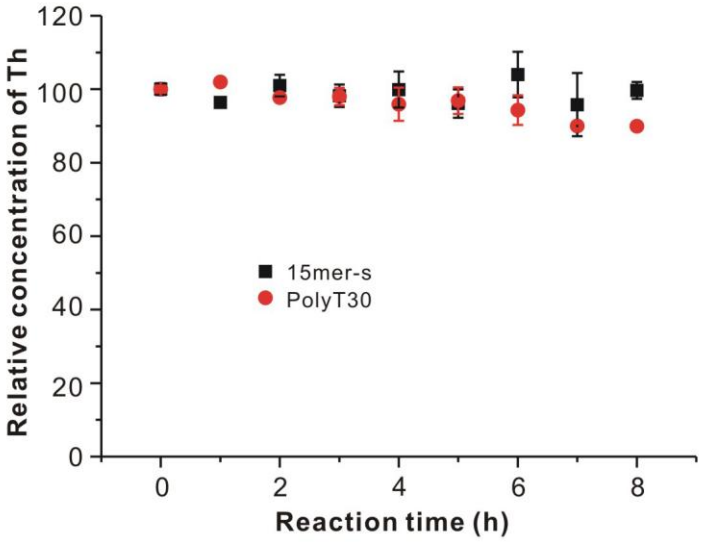

Figure 3-8. Illustration of sequence specific nanozymes (three-base modified 15mer-thrombin aptamer, 15mer-s, GGT-TGG-TGT-GGT-AAA-T20; and PolyT30) that display no-degradation to thrombin.

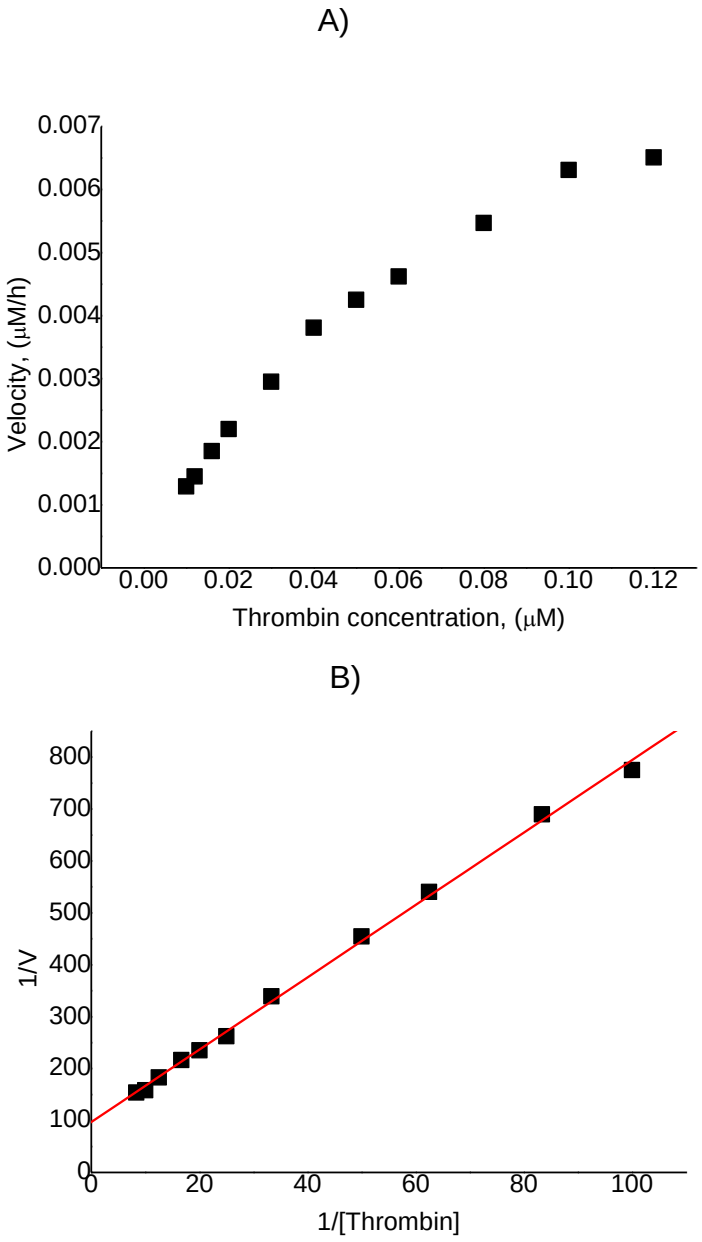

Figure 3-9. Enzyme kinetics of nanozyme. A) thrombin concentration versus nanozyme reaction velocity. B) Lineweaver-Burke plot of thrombin selective nanozyme.

A)

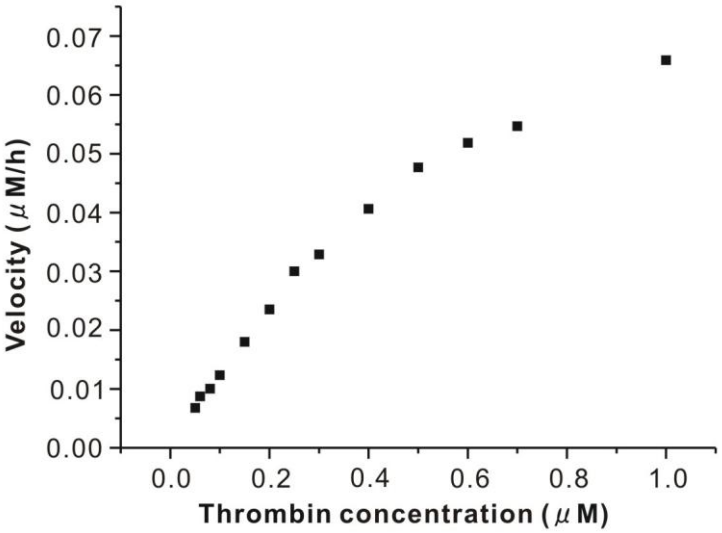

B)

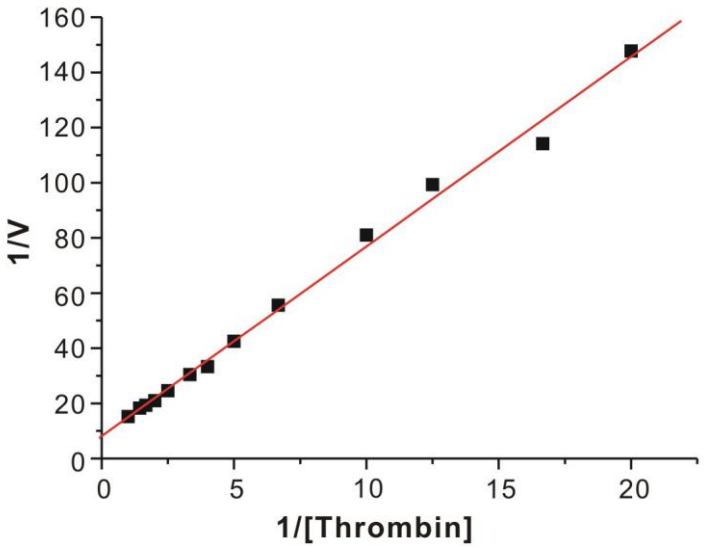

Figure 3-10. Enzyme kinetics of native proteinase K. A) thrombin concentration versus native proteinase K reaction velocity. B) Lineweaver-Burke plot of native proteinase K.

Table 3-2. Nanozyme and native proteinase K kinetic constants

Kinetic constants	Nanozyme	Native proteinase K
K_m (μM)	0.072	0.845
V_{max} (μM/h)	0.010	0.123
k_{cat} (/s)	0.003	0.034
K_{cat}/k_m (/s·M)	44,282	40,393

The equation of Lineweaver-Burke plot for nanozyme, Y=6.97+97.19, R=0.9991; for native proteinase K, Y=6.88X+8.13, R=0.9994.

CHAPTER 5
ON-OFF SWITCH AVAILABLE NANOPARTICLE-BASED CELLULAR MACHINERY FOR THE DEGRADATION OF SPECIFIC PROTEIN

If physicians are able to control the activity of therapeutic agents rapidly when they do surgeries, patient safety could be enhanced. Using an antidote is the safest way to control the activity of drugs because regulation of the therapeutic agent activity is not relies on the patient physiology unlikely rapid removing drugs.

Coagulation disorders are highly related to many serious diseases including heart attacks and strokes[43]. Because thrombin can form blood clots, thrombin, consequently, became a typical target protein for anti-coagulation therapies for cardiovascular, cerebrovascular and peripheral vascular disease[44-46].

In 2006, the American Heart Association reported that prevalence rate of coronary heart disease were 17.6M in the United States[50]. As an important enzyme in the coagulation process, thrombin activity is an issue during coronary artery bypass surgery, percutaneous coronary intervention and heart transplantations. And, an anti-thrombin agent or agent that is able to inhibit thrombin activity has been used as an anti-coagulant during these surgeries. However, the bleeding and its treatment are difficulties to get successful outcome and cost for patient treatment.

The ideal anti-coagulants should meet the demands for immediately therapeutic, not to need frequent monitoring from the easy dosing and immediately reversible so that it could be predictable.

Heparin is the most common anti-coagulant which can bind to exosite II on thrombin, and then it indirectly inhibits thrombin activity, because heparin strongly catalyzes the function of anti-thrombin[51]. Since heparin must be used with the antidote protamine, heparin-protamine treatment leads to a number of side-effects including

bleeding and platelet count reduction. In addition, heparin has a number of disadvantages including non-specific binding to plasma proteins, unable to inhibit clot-bound thrombin and dosing difficulty due to non-linear kinetics[52, 53]. Thus, there is a demand for a development of safe, long-lasting and moderate-cost anti-coagulant which is not associated with the side effects.

From the demands that have been mentioned above, we developed the nanoparticle-based cellular machinery for the degradation of thrombin. However, because of not to have on/off switch function, it would have limitations to be used for an anti-coagulant at real system.

For future research, I would propose the on/off switch available nanoparticle-based cellular machinery for the degradation of thrombin by adapting antidote control.

Rusconi, C. P. *et al* (Nature Biotechnology, **2004**)[53] and Nimjee, S. M. *et al* (Molecular Therapy, **2006**)[52] have investigated aptamer based antidote-mediated control for an anti-coagulant *in vivo*. They used the factor IXa aptamer as an anti-coagulant, and then synthesized the base-pairing antidote (Figure 4-1). Consequently, active anti-congualant factor IXa aptamer was inactivated by synthesized antidote which regulated aptamer function.

Harris, D. C *et al* (JACS, **2008**)[97] have proposed the idea of DNA-small molecule chimera with responsive protein-binding ability. To control the binding affinity to trypsin, they modified two each ends of 15mer-thrombin aptamer (GGT-TGG-TGT-GGT-TGG) with exosite binder and active site binder which consist of small molecules. High affinity complex was exhibited by bidentate interactions through DNA-small molecule chimera, whereas, duplex bound to two molecules of trypsin would be expected to have low

affinity binding to trypsin. To open the folded 15mer-thrombin aptamer, they introduced the CCA-ACC-ACA-CCA-ACC capable of forming Watson-Crick base pairs (Figure 4-2).

From these two ideas I would propose on/off switch available anti-thrombin therapeutic agent by simply adapting the use of Watson-Crick base pairs (CCA-ACC-ACA-CCA-ACC) for future research (Figure 4-3). By adding adequate amount of base pairs for anti-thrombin nanozyme antidote, safe, long-lasting and moderate-cost anti-coagulant which is not associated with the side effects would be developed. Furthermore, unlikely heparin - nonspecific binding to plasma proteins and dosing difficulty due to non-linear kinetics – antithrombin nanozyme would show the extremely high specific to thrombin and linear kinetics due to thrombin degradation from proteinase K so that easy and predictable dosing of anti-thrombin drugs would be possible.

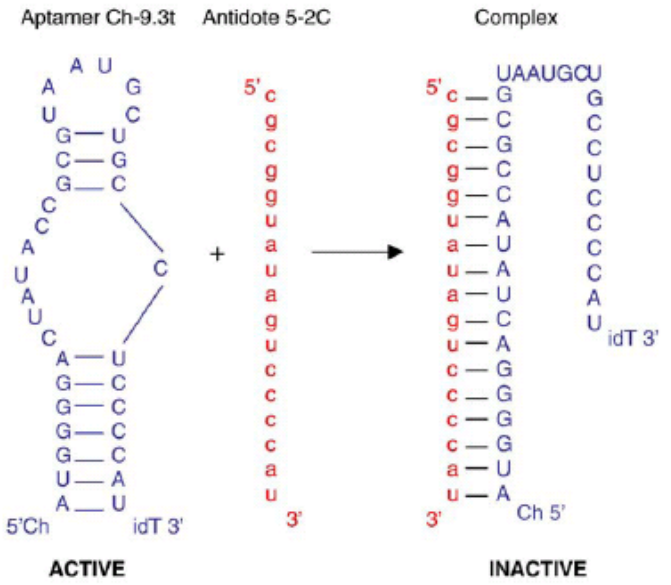

Figure 4-1. Predicted secondary structure of anti-FIXa aptamer and its interaction with antidote to control aptamer function.

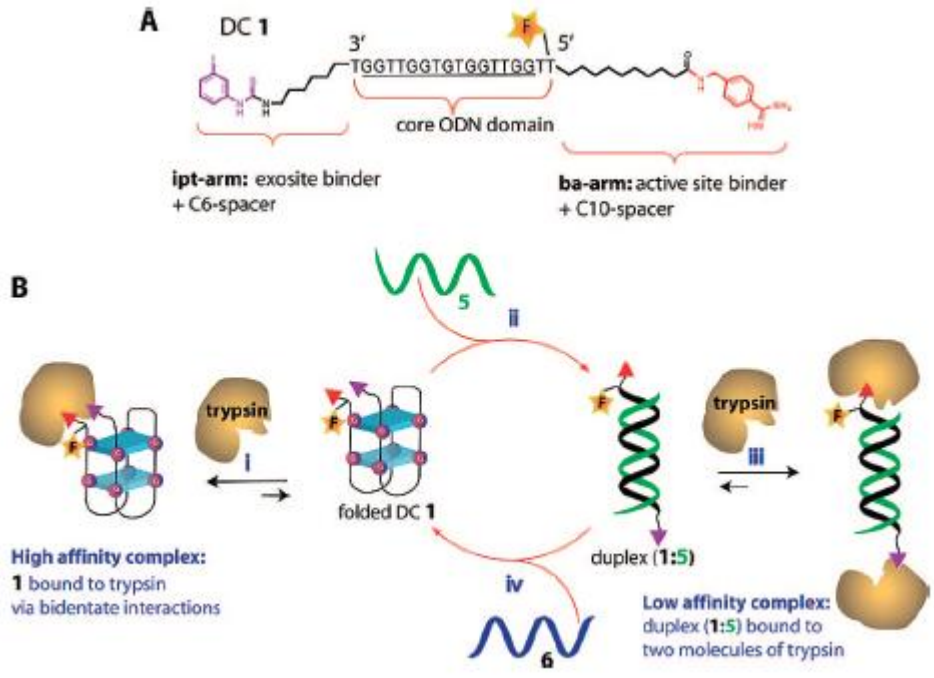

Figure 4-2. (A) Design of DNA-small molecule chimera. (B) Controlled trypsin-binding through addition of external oligonucleotide-derived stimuli.

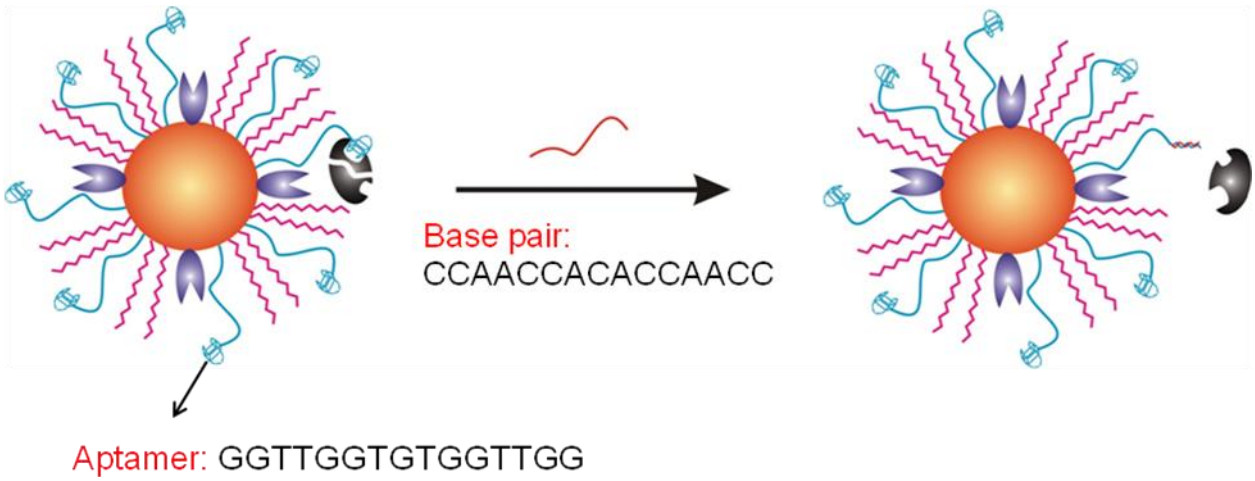

Figure 4-3. Scheme of anti-thrombin nanozyme antidote control.

LIST OF REFERENCES

1. Brigger, I.; Dubernet, C.; Couvreur, P. *Adv. Drug. Deliver. Rev.* **2002**, *54*, 631-651.

2. Peer, D.; Karp, J. M.; Hong, S.; Farokhzad, O. C.; Margalit, R.; Langer, R. *Nat. Nanotechnol.* **2007**, *2*, 751-760.

3. Duncan, B.; Kim, C.; Rotello, V. M. *J. Control Release* **2010**, *148*, 122-127.

4. Chan, W. C. W.; Nie, S. M. *Science* **1998**, *281*, 2016-2018.

5. Wu, W.; Li, A. D. *Nanomedicine (Lond)* **2007**, *2*, 523-531.

6. Song, H. M.; Wei, Q. S.; Ong, Q. K.; Wei, A. *ACS Nano* **2010**, *4*, 5163-5173.

7. Graham, D.; Faulds, K. *Expert. Rev. Mol. Diagn* **2009**, *9*, 537-539.

8. Han, G.; Ghosh, P.; De, M.; Rotello, V. M. *Nanobiotechnol* **2007**, *3*, 40-45.

9. Ghosh, P.; Han, G.; De, M.; Kim, C. K.; Rotello, V. M. *Advanced Drug Delivery Reviews* **2008**, *60*, 1307-1315.

10. Hill, R. T.; Shear, J. B. *Anal. Chem*. **2006**, *78*, 7022-7026.

11. Simonian, A. L.; Good, T. A.; Wang, S. S.; Wild, J. R. *Anal. Chim. Acta* **2005**, *534*, 69-77.

12. Elghanian, R.; Storhoff, J. J.; Mucic, R. C.; Letsinger, R. L.; Mirkin, C. A. *Science* **1997**, *277*, 1078-1081.

13. Taton, T. A.; Mirkin, C. A.; Letsinger, R. L. *Science* **2000**, *289*, 1757-1760.

14. Taton, T. A.; Lu, G.; Mirkin, C. A. *J. Am. Chem. Soc.* **2001**, *123*, 5164-5165.

15. Pathak, S.; Choi, S. K.; Arnheim, N.; Thompson, M. E. *J. Am. Chem. Soc.* **2001**, *123,* 4103-4104.

16. He, L.; Musick, M. D.; Nicewarner, S. R.; Salinas, F. G.; Benkovic, S. J.; Natan, M. J.; Keating, C. D. *J. Am. Chem. Soc.* **2000**, *122,* 9071-9077.

17. Li, Z.; Jin, R.; Mirkin, C. A.; Letsinger, R. L. *Nucleic Acids Research*, **2002**, *30*, 1558-1562.

18. Cassileth, B. R. *Enzyme Therapy In The Alternative Medicine Handbook*. New York: W.W. Norton & Company, **1998**.

19. Cichoke, A. J. *Enzymes & Enzyme Therapy: How to Jump-Start Your Way to Lifelong Good Health* Chicago: Keats Publishing, **2000**.

20. Roxas, M. *Alternative Medicine Review*, **2008**, *13*, 307-314.

21. Smith, M. J.; Beekhuis, H.; Duursma, A. M.; Bouma, J. M.; Gruber, M. *Clin. Chem*. **1998**, *34*, 2475-2480.

22. Mello, C. C. *Angew. Chem. Int. Ed.* **2007**, *46*, 6985-6994.

23. Alberts, B. *Molecular biology of the cell*. 5th Edn, (Garland Science, **2008**).

24. Castanotto, D.; Rossi, J. J. *Nature* **2009**, *457*, 426-433.

25. Davis, M. E.; Zuckerman . J. E.; Choi, C. H.; Seligson, D.; Tolcher, A.; Alabi, C. A.; Yen, Y.; Heidel, J. D.; Ribas. A. *Nature* **2010**, *464*, 1067-1070.

26. Grimm, D.; Streetz, K. L.; Jopling, C. L.; Storm, T. A.; Pandey, K.; Davis, C. R.; Marion, P.; Salazar, F.; Kay, M. A. *Nature* **2006**, *441*, 537-541.

27. Kurreck, J. *Angew. Chem. Int. Ed.* **2009***, 48*, 1378-1398.

28. Ji, J.; Glaser, A.; Wernli, M.; Berke, J. M.; Moradpour, D.; Erb, P. *J. Gen. Virol.* **2008**, *89*, 2761-2766.

29. Triboulet, R.; Mari, B.; Lin, Y.; Chable-Bessia, C.; Bennasser, Y.; Lebrigand, K.; Cardinaud, B.; Maurin, T.; Barbry, P.; Baillat, V.; Reynes, J.; Corbeau, P.; Jeang, K.; Benkirane, M. *Science* **2007**, *315*, 1579-1582.

30. Park, S. J.; Taton, T. A.; Mirkin, C. A. *Science* **2002**, *295*, 1503-1506.

31. Rosi, N. L.; Giljohann, D. A.; Thaxton, C. S.; Lytton-Jean, A. K. R.; Han, M. S.; Mirkin, C. A. *Science* **2006**, *312*, 1027-1030.

32. Tsai, W. L.; Chung, R. T. *Oncogene* **2010**, *29*, 2309-2324.

33. Lanford, R. E.; Hildebrandt-Eriksen, E. S.; Petri, A.; Persson, R.; Lindow, M.; Munk, M. E.; Kauppinen, S.; Qrum, H. *Science* **2010**, *327*, 198-201.

34. Ploss, A.; Rice, C. M. *EMBO Rep.* **2009**, *10*, 1220-1227.

35. McMullan, L. K.; Grakoui, A.; Evans, M. J.; Mihalik, K.; Puig, M.; Bransh, A. D.; Feinstone, S. M.; Rice, C. M. *Proc. Natl. Acad. Sci. U.S.A.* **2007**, *104*, 2879-2884.

36. Yokota, T.; Sakamoto, N.; Enomoto, N.; Tanabe, Y.; Miyagishi, M.; Meakawa, S.; Yi, L.; Kurosaki, M.; Taira, K.; Watanabe, M.; Mizusawa, H. *EMBO Rep.* **2003**, *4*, 602-608.

37. Grabar, K. C.; Freeman, R. G.; Hommer, M. B.; Natan, M. J.; *Anal. Chem.* **1995**, *67,* 735-743.

38. Bendayan, M. *J. Histochem. Cytochem.* **1981**, *29*, 531.

39. Bendayan, M. The enzyme-gold cytochemical approach: a review, chap. 8 in Hayat, M. A. *Colloid gold: principles, methods, and applications.* (Academic Press, San Diego, **1989**) vol. 2.

40. Wakita, T.; Pietschmann, T.; Kato, T.; Date, T.; Miyamoto, M.; Zhao, Z.; Murthy, K.; Habermann, A.; Kräusslich, H.-G.; Mizokami, M.; Bartenschlager, R.; Liang, T. J.; *Nature Med.* **2005**, 11, 791-796.

41. Kelly, B. M.; Yu, C. Z.; Chang, P. L. *Eur. J. Cell. Biol.* **1989**, *48*, 71-78.

42. Changeux, J. P.; Edelstein, S. J. *Science* **2005**, *308*, 1424-1428.

43. Dahlbäck, B. *Lancet* **2000**, *355* , 1627-1632.

44. Gopinath, S. C. B. *Thromb. Res.* **2008**, *122*, 838-847.

45. Petrera, N. S.; Stafford, A. R.; Leslie, B. A.; Kretz, C. A.; Fredenburgh, J. C.; Weitz, J. I. *J. Biol. Chem.* **2009**, *284*, 25620-25629.

46. Ginsberg, J. A.; Crowther, M. A.; White, R. H.; Ortel, T. L. *Hematology* **2001**, 2001, 339-357.

47. Rodgers, G. M. *Thromb. Haemost*. **2009**, *101*, 806-812.

48. Tracy, R. P. *CHEST* **2003**, *124*, 49-57.

49. Donavan, F. M.; Pike, C. J.; Cotman, C. W.; Cunningham, D. D. *The Journal of Neuroscience* **1997**, *17*, 5316-5326.

50. *Heart Disease & Stroke Statistics*, American Heart Association, **2010**.

51. Nisio, M. D.; Middeldorp, S.; Buller, H. R. *The New England Journal of Medicine* **2005**, *353*, 1028-1040.

52. Nimjee, S. M.; Keys, J. R.; Pitoc, G. A.; Quick, G.; Rusconi, C. P.; Sullenger, B. A. *Mol. Ther.* **2006**, *14*, 408-415.

53. Rusconi, C. P.; Roberts, J. D. Pitoc, G. A.; Nimjee, S. M.; White, R. R.; Quick, G., Jr.; Scardino, E.; Fay, W. P.; Sullenger, B. A. *Nat. Biotechnol.* **2004**, *22*, 1423-1428.

54. Joachimi, A.; Mayer, G.; Hartig, J. S. *J. Am. Chem. Soc*. **2007**, *129*, 3036-3037.

55. Heckel, A.; Mayer, G. *J. Am. Chem. Soc*. **2005**, *127*, 822-823.

56. Kim. Y.; Cao, Z.; Tan. W *Proc. Natl. Acad. Sci* **2008**, *105*, 5664-5669.

57. Wolberg, A. S. *Blood Rev.* **2007**, *21* , 131-

58. Berliner, L. J. *Molecular and Cellular Biochemistry* **1984**, *61*, 159-172.

59. Mann, K. G.; Lundblad, R. L. *Hemostasis and thrombosis: basic principles and clinical practice*. J. B. Lippincott Co., Philadelphia **1987**.

60. Linkins, L.; Weitz, J. I. *Annu. Rev. Med.* **2005**, 56, 63-77.

61. Fernindez-Romero, J.M.; Castro L. *Talanta* **1996**, 43, 1531-1537.

62. Nishno, A.; Suzuki, M.; Ohtani, H.; Motohashi, O.; Umezawa, K.; Nagura, H.; Yoshimoto, T. *J. of Neurotrauma* **1993**, *10,* 167-179.

63. Arai, T.; Miklossy, J.; Andis, K.; Guo, J.; McGeer P. L. *J Neuropathol Exp Neurol* **2006,** *65,* 19-25.

64. Cera, E. D.; Dang, Q. D.; Ayala, Y. M. *Cellular and Molecular Life Sciences* **1997**, *53*, 701-730.

65. Bode, W.; Turk, D.; Karshikov, A. *Protein Science* **1992**, *1*, 426-471.

66. Lesk, A. M.; Fordham, W. D. *Journal of Molecular Biology* **1996**, *258*, 501-537.

67. Cera, E. D. *Mol. Aspects Med.* **2008**, *29*, 203-254.

68. Becker, R. C.; Spencer, F. A. *J. Thromb. Thrombolysis* **1998**, *5*, 215-229.

69. Rose, T.; Cera, E. D. *J. Biol. Chem.* **2002** , *277* , 18875-18880.

70. Tsiang, M.; Jain, A. K.; Dunn, K. E.; Rojas, M. E.; Leung, L. L. K. ; Gibbs, C. S. *J. Biol. Chem.* **1995** , *270* , 16854-16863.

71. Tuerk, C.; Gold, L. *Science* **1990**, *249*, 505-510.

72. Ellington, A. D.; Szostak, J. W. *Nature* **1990**, *346*, 818-822.

73. Mayer, G. *Angew. Chem. Int. Ed.* **2009** , *48* , 2672-2689.

74. Barbas, A. S.; White, R. R. *Curr. Opin. Invest. Drugs* **2009**, *10*, 572-578.

75. Thiel, K. W.; Giangrande, P. H.; *Oligonucleotides* **2009**, *19*, 209-222.

76. Bock, L. C.; Griffin, L. C.; Latham, J. A.; Vermaas, E. H.; Toole, J. J. *Nature* **1992**, *355*, 564-566.

77. Griffin, L. C.; Tidmarsh, G. F.; Bock, L. C.; Toole, J. J.; Leung, L. L. *Blood* **1993**, *81*, 3271-3276.

78. Huizenga, D. E.; Szostak, J. W. *Biochemistry* **1995**, *34*, 656-665.

79. Stojanovic, M. N.; Prada, P.; Landry D. W. *J. Am. Chem. Soc*. **2001**, *123*, 4928-4931.

80. Hamaguchi N.; Ellington A.; Stanton, M. *Analytical Biochemistry* **2001**, *294*, 126-131.

81. Yamamoto, R.; Kumar, P. K. R. *Genes to Cells* **2000**, *5*, 389-396.

82. German, I.; Buchanan, D. D.; Kennedy, R. T. *Anal. Chem*. **1998**, *70*, 4540-4545.

83. Berezovski, M.; Nutiu, R.; Li, Y.; Krylov, S. N. *Anal. Chem.* **2003**, *75*, 1382-1386.

84. Xiao, Yi.; Lubin, A. A.; Heeger, A. J.; Plaxco, K. W. *Angew. Chem. Int. Ed*. **2005**, *44*, 5456-5459.

85. Radi, A.; Sa´nchez, J. L. A.; Baldrich. E.; O'Sullivan, C. K. *J. Am. Chem. Soc*. **2006**, *128*, 117-124.

86. Nutiu, R.; Li, Y. *Chem. Eur. J*. **2004**, *10*, 1868-1876.

87. Nutiu, R.; Li, Y. *J. Am. Chem. Soc*. **2003**, *125*, 4771-4778.

88. Pavlov, V.; Xiao Y.; Shlyahovsky, B., Willner, I. *J. Am. Chem. Soc*. **2004**, *126*, 11768-11769.

89. Ho, H.; Leclerc, M. *J. Am. Chem. Soc*. **2004**, *126*, 1384-1387.

90. Xu, H.; Mao, X.; Zeng, Q.; Wang, S.; Kawde, A.; Liu, G. *Anal. Chem.* **2009**, *81*, 669-675.

91. Cho H.; Baker, B. R.; Wachsmann-Hogiu S.; Pagba C. V.; Laurence, Ted. A.; Lane S. M.; Lee L. P.; Tok J. B.-H. *Nano Letters* **2008**, *9*, 4386-4390.

92. Hu J.; Zheng, P.-C., Jiang, J.-H.; Shen, G.-L., Yu, R.-Q.; Liu, G.-K. *Anal. Chem*. **2009**, *81*, 87-93.

93. Buschmann, A.; Kuczius, T.; Bodemer, W.; Groschup, M. H. *Biochem. Biophys. Res. Commun*. **1998**, *253*, 693-702.

94. Pahler, A.; Banerjeel, A.; Dattaguptal, J.K.; Fujiwaral, T.; Lindner, K.; Pal, G.P.; Suck, D.; Weber, G.; Saenger, W. *EMBO* **1984**, *3*, 1311-1314.

95. Yoshimoto, M.; Wang, S.; Fukunaga, K.; Treyer, M.; Walde, P.; Kuboi, R.; Nakao, K. *Biotechnology and Bioengineering* **2004**, *85*, 222-233.

96. Slovakova, M.; Peyrin, J. –M.; Bilkova, Z.; Juklickova, M.; Hernychova, L.; Viovy, J. –L. *Bioconjugate Chem.* **2008**, *19*, 966-972.

97. Harris, D. C.; Chu, X.; Jayawickramarajah, J. *J. Am. Chem. Soc.* **2008**, *130*, 14950-14951.

BIOGRAPHICAL SKETCH

Soon Hye Yang earned her Master of Science degree in chemistry from the University of Florida in 2011 and Kwangwoon University in Seoul 2007. She received her Bachelor of Science in chemistry from Kwangwoon University in Seoul 2005.